

*Carnegie Observatories Astrophysics Series, Vol. 3:  
 Clusters of Galaxies: Probes of Cosmological Structure and Galaxy Evolution  
 ed. J. S. Mulchaey, A. Dressler, and A. Oemler (Pasadena; Carnegie Observatories:  
<http://www.ociw.edu/ociw/symposia/series/symposium3/proceedings.html>)*

---

# The Environmental Effects on Galaxy Evolution Based on the SDSS Data

Tomotsugu Goto, the Pittsburgh Astrophysics group, and the SDSS collaboration  
*Department of Astronomy, Graduate School of Science, The University of Tokyo  
 7-3-1 Hongo, Bunkyo-ku, Tokyo 113-0033, Japan  
 yohnis@icrr.u-tokyo.ac.jp*

---

## Abstract

By constructing a large, uniform galaxy cluster catalog from the SDSS data, we have found that cluster galaxies evolve both spectrally and morphologically. By studying the morphology–cluster-centric-radius relation, we have found two characteristic environments where galaxy morphologies change dramatically. We found passive spiral galaxies in the infalling region of clusters. They are likely to be a galaxy population in transition due to the cluster environment. We also studied E+A galaxies, which have also been thought to be cluster originated. We found that E+As live in all environments including the field region.

## 1.1 Introduction: the Sloan Digital Sky Survey

The Sloan Digital Sky Survey (SDSS; York et al. 2000) is both an imaging and spectroscopic survey of a quarter of the sky. Imaging part of the survey takes CCD images of the sky in five optical bands ( $u, g, r, i$  and  $z$ ; Fukugita et al. 1995). The spectroscopic part of the survey observes one million galaxies. We use this excellent data set to tackle the long standing problems on environmental effects on galaxy evolution. The cosmological parameters adopted are  $H_0=75$  km s<sup>-1</sup> Mpc<sup>-1</sup>, and  $(\Omega_m, \Omega_\Lambda, \Omega_k)=(0.3, 0.7, 0.0)$ .

## 1.2 The SDSS Cut & Enhance Galaxy Cluster Catalog

The SDSS Cut & Enhance galaxy cluster catalog (CE; Goto et al. 2002a) is one of the initial attempts to produce a cluster catalog from the SDSS imaging data. It uses generous color-cuts to eliminate fore- and background galaxies when detecting clusters. Its selection function is calculated using a Monte Carlo simulation. The accuracy of photometric redshift is  $\Delta z=0.015$  at  $z<0.3$ . Composite luminosity functions of clusters are studied in Goto et al. (2002b).

## 1.3 The Morphological Butcher-Oemler Effect

Utilizing the SDSS CE cluster catalog, we studied spectral and morphological evolution of cluster galaxies (Goto et al. 2003a). In the left panels of Fig.1.1 fractions of blue galaxies are plotted against redshift. Lines and stars show the best-fit and medians. In the lower panel, the definition of blue galaxies is by 0.2 bluer than red-sequence in  $g-r$ . In the upper panel, a galaxy with  $u-r<2.2$  is called blue. In both panels, higher redshift clusters show larger fractions of blue galaxies (the Butcher-Oemler effect). In right panels, fractions

of spiral galaxies are plotted as a function of redshift. In the upper panel, concentration is used to separate spiral galaxies. In the lower panel, profile fit is used. In both panels, higher redshift clusters show higher fractions of spiral galaxies (the morphological Butcher-Oemler effect). Throughout the panels in Fig.1.1, large scatter can be recognized in addition to the redshift evolution. To investigate, we plot the difference from the best-fit line against cluster richness in Fig.1.2. All panels show slight signs of decreasing blue fractions with increasing richness. The trend is consistent with the ram-pressure stripping model discussed in Fujita et al. (1999).

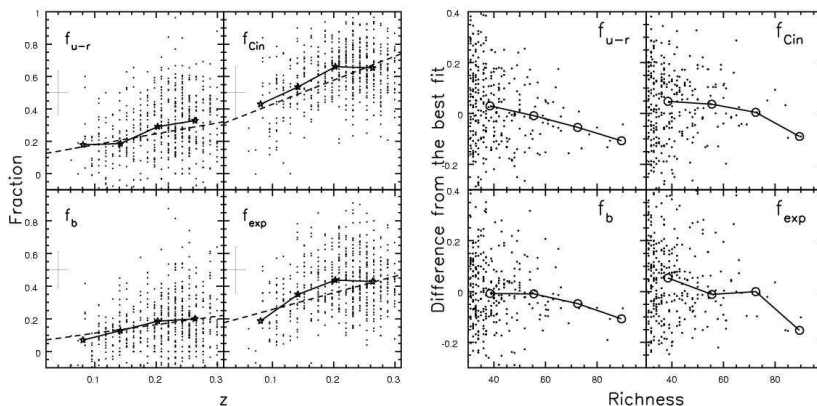


Fig. 1.1. (left) Photometric and morphological Butcher-Oemler effect from the 514 SDSS Cut & Enhance galaxy clusters. Blue fractions ( $f_b$ ,  $f_{u-r}$ ) and spiral fractions ( $f_{Cin}$ ,  $f_{exp}$ ) are plotted against redshift. The dashed lines show the weighted least-squares fit to the data. The stars and solid lines show the median values. The median values of errors are shown in the upper left corners of each panel. The Spearman’s correlation coefficients show highly significant correlation in all cases.

Fig. 1.2. (right) The difference of the late-type fractions from the best fit lines as a function of redshift are plotted against cluster richness. Solid lines and circles show the median values.

#### 1.4 The Morphology–Cluster-Centric-Radius Relation

Using a volume limited sample of 7938 spectroscopic galaxies ( $0.05 < z < 0.1$ ,  $Mr < -20.5$ ), we investigated the morphology–cluster-centric-radius relation in the SDSS (Goto et al. 2003b). We classified galaxies using the *Tauto* method, which uses concentration and coarseness of galaxies (see Yamauchi et al. 2003 for more details of *Tauto*). We measured the distance to the nearest cluster using the C4 cluster catalog (Miller et al. 2003). In Fig.1.3, morphological fractions of E, S0, Sa and Sc galaxies are shown in red, green, cyan and blue as a function of cluster-centric-radius. Around  $1 R_{vir}$ , fractions of Sc start to decrease. Around  $0.3 R_{vir}$ , S0 starts to decrease and E starts to increase. These two changes imply there might be two different physical mechanisms responsible for cluster galaxy evolution. Since a physical size of S0 galaxies ( $Tauto=0$ ) is smaller than E and Sc ( $Tauto=2$  and  $-1$ ) in Fig.1.4, the results are consistent with the hypothesis that in the outskirts, stripping

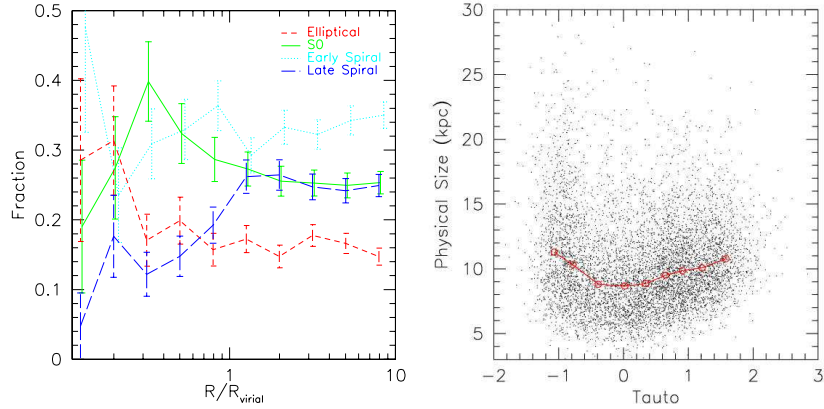


Fig. 1.3. (left) The morphology-radius relation. Fractions of each type of galaxies are plotted against cluster-centric-radius to the nearest cluster. Short-dashed, solid, dotted and long-dashed lines represent elliptical, S0, early-spiral and late-spiral galaxies classified with the automated method, respectively.

Fig. 1.4. (right) Physical sizes of galaxies are plotted against  $T_{\text{auto}}$ . Petrosian 90% flux radius in  $r$  band is used to calculate physical sizes of galaxies. A solid line shows medians. It turns over around  $T_{\text{auto}} \sim 0$ , corresponding to S0 population.

creates small S0 galaxies from spiral galaxies and, in the cluster cores, the merging of S0s results in a large Es.

## 1.5 The Passive Spiral Galaxies

In the same volume limited sample of the SDSS, we have found an interesting class of galaxies with spiral morphologies (Fig. 1.5), and without any star formation activity (shown by the lack of emission lines in the spectrum; Fig. 1.6). More interestingly, these galaxies exist in the infalling region of clusters ( $1 \sim 10 R_{\text{vir}}$  or  $1 \sim 2 \text{ Mpc}^{-2}$ ; Fig.1.7, Fig.1.8). These passive spiral galaxies might be the population of galaxies in transition between blue/spiral and red/S0 galaxies. Details are given in Goto et al. (2003c)

## 1.6 E+A Galaxies

We selected E+A galaxies in the SDSS as galaxies with  $H\delta \text{ EW} < 4 \text{ \AA}$  and no detection of [OII] and  $H\alpha$  (Goto et al. 2003d). E+A galaxies have strong Balmer absorption lines but no emission lines which indicate star formation activity. These features are interpreted as a post-starburst signature and people have speculated that cluster related phenomena might cause the truncation of starburst. Interestingly, however, we have found a contrasting result in Fig.1.9, where the density distribution of E+As is statistically consistent with that of the field galaxies. Morphologically, several E+A galaxies found in the past showed disc-like morphology. However in our data, most of E+As show elliptical-like morphology (Fig.1.10). Another possible explanation of E+As is dust-hidden star forming galaxies. However in Fig.1.11, E+As do not look dustier.

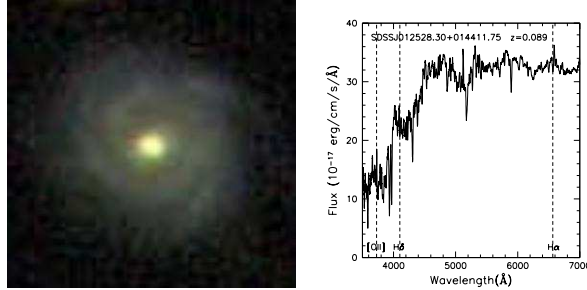


Fig. 1.5. (left) An example image of a passive spiral galaxy. The image is a composite of SDSS  $g$ ,  $r$  and  $i$  bands, showing  $30'' \times 30''$  area of the sky with its north up. Discs and spiral arm structures are recognized.

Fig. 1.6. (right) An example restframe spectrum of the passive spiral galaxy. Spectrum is shifted to restframe and smoothed using a  $10\text{\AA}$  box. The image is shown in Fig. 1.5.

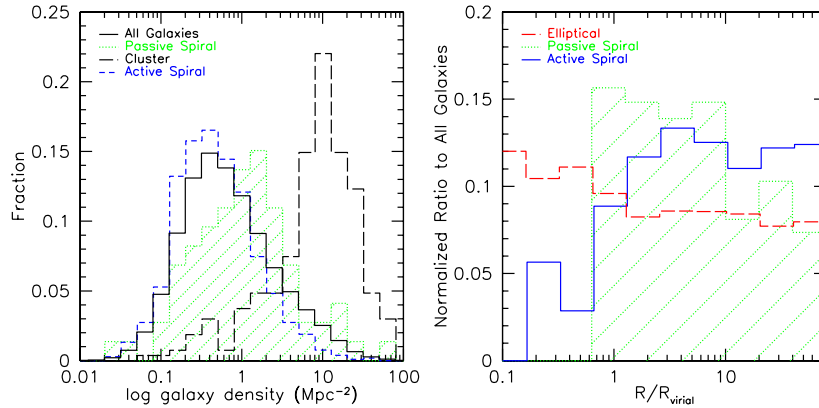


Fig. 1.7. (left) The density distribution of passive spiral galaxies (hashed region) and all galaxies (solid line) in a volume limited sample. Local galaxy density is measured based on the distance to the 5th nearest galaxy within  $\pm 3000$  km/s. A Kolomogorov-Smirnov test shows distributions of passive spirals and all galaxies are significantly different. A long dashed line shows the distribution of cluster galaxies. A short dashed line shows that of active spiral galaxies. Both of them are statistically different from that of passive spirals.

Fig. 1.8. (right) The distribution of passive spiral galaxies as a function of cluster-centric-radius. A solid, dashed and dotted lines show the distributions of passive spiral, elliptical and active spiral galaxies, respectively. The distributions are relative to that of all galaxies in the volume limited sample and normalized to be unity for clarity. The cluster-centric-radius is measured as a distance to a nearest C4 cluster (Miller et al. 2003) within  $\pm 3000$  km/s, and normalized by virial radius (Girardi et al. 1998).

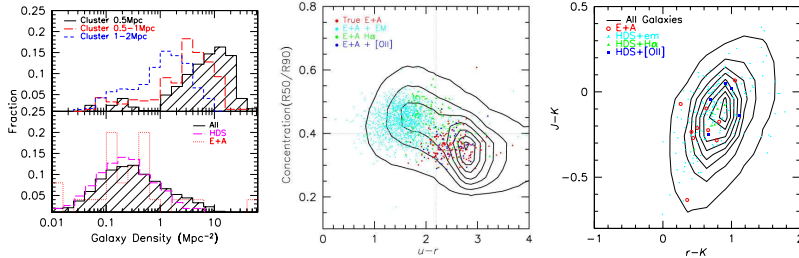


Fig. 1.9. (left) Local galaxy density distribution. The upper panel shows the density distribution of cluster galaxies for comparison. In the lower panel, red, magenta and black histograms show the density distributions of E+A, H $\delta$ -strong (HDS) and all galaxies, respectively. According to a Kolomogorov-Smirnov test, the distributions of E+A and cluster galaxies are significantly different.

Fig. 1.10. (middle) A concentration parameter  $Cin$  is plotted against  $u-r$  color. The concentration parameter ( $Cin$ ) is defined as the ratio of Petrosian 50% light radius to Petrosian 90% light radius in  $r$  band (radius which contains 50% and 90% of Petrosian flux, respectively). The contours show the distribution of all galaxies in our sample. The distribution shows two peaks, one for elliptical galaxies at around  $(u-r, Cin)=(2.8, 0.35)$ , and one for spiral galaxies at around  $(u-r, Cin)=(2.0, 0.45)$ . Red, blue, green, and cyan dots show the distribution of E+A, HDS+[OII] emission, HDS+H $\alpha$  emission and HDS+both emission galaxies, respectively.

Fig. 1.11. (right) Restframe  $J-K$  color is plotted against  $r-K$ . The contours show the distribution of all galaxies in our sample. Symbols are the same as the middle panel. E+A galaxies are not much redder than normal galaxies, suggesting they are not dustier systems.

## 1.7 Conclusions

By constructing a large, uniform galaxy cluster catalog from the SDSS data, we have found that cluster galaxies evolve both spectrally (the Butcher-Oemler effect) and morphologically (the morphological Butcher-Oemler effect). By studying the morphology–cluster-centric-radius relation, we have found two characteristic environment where galaxy morphology changes dramatically, suggesting the existence of two different physical mechanisms in cluster regions. Passive spiral galaxies are likely to be a galaxy population in transition due to the cluster environment. Although E+A galaxies have been thought to be cluster related, we found E+As in the field. These field E+As can not be explained by the cluster environment.

## References

- Fukugita, M., Shimasaku, K., & Ichikawa, T. 1995, *PASP*, 107, 945  
 Fujita, Y. & Nagashima, M. 1999, *ApJ*, 516, 619  
 Girardi, M., Giuricin, G., Mardirossian, F., Mezzetti, M., & Boschin, W. 1998, *ApJ*, 505, 74  
 Goto, T. et al. 2002a, *AJ*, 123, 1807  
 Goto, T. et al. 2002b, *PASJ*, 54, 515  
 Goto, T. et al. 2003a, *PASJ*, 55, 739

*T. Goto et al.*

Goto, T. et al. 2003b, MNRAS, 346, 601

Goto, T. et al. 2003c, PASJ, 55, 757

Goto, T. et al. 2003d, PASJ, 55, 771

Miller, C. et al. 2004, in prep.

Yamauchi, C. et al. 2004, in prep.

York, D. G. et al. 2000, AJ, 120, 1579